

Based on the Dual Pathway of Interaction-Mediated NF- κ B in Cell Apoptosis and Immune Inflammation to Study the Effect of Danzhi Xiaoyao Powder on the Learning and Cognitive Ability of AD Model Rats

Hu-Ping Wang^{1-3*}, Ming-Cheng Li^{4*}, Jiao Yang¹, Jun Zhou⁵, Zhi-Peng Meng¹, Yun-Yun Hu¹, Yu-Jie Lyu¹, Yi-Qin Chen¹, Yu-Mei Han¹, Wen-Li Pei¹

¹School of Basic Medicine, Gansu University of Traditional Chinese Medicine, Lanzhou, People's Republic of China; ²Key Laboratory of Traditional Chinese Herbs and Prescription Innovation and Transformation of Gansu Province, Gansu University of Traditional Chinese Medicine, Lanzhou, People's Republic of China; ³Laboratory for TCM New Products Development Engineering of Gansu Province, Lanzhou, People's Republic of China; ⁴Qujing 69 Hospital, China RongTong Medical Healthcare Group Co. Ltd., Qujing, People's Republic of China; ⁵Preventive Medicine Department, Xichang Hospital of Traditional Chinese Medicine, Xichang, People's Republic of China

*These authors contributed equally to this work

Correspondence: Hu-Ping Wang, Gansu University of Traditional Chinese Medicine, 35 Dingxi East Road, Lanzhou, People's Republic of China, Email whp@gszy.edu.cn

Background: Apoptosis and immune inflammation play important roles in the pathological process of Alzheimer's disease (AD), but their specific pathogenesis is still unclear. Therefore, this article focuses on exploring the effects of Danzhi Xiaoyao Powder (DXP) on the learning and memory ability of AD model rats from the dual mechanisms of apoptosis and immune inflammation.

Methods: The AD model was replicated by injecting Okadaic acid (100 ng) into the bilateral hippocampus of rats. Successful rats were selected and orally administered with donepezil hydrochloride and DXP decoction for 42 days. Their learning and memory abilities, hippocampal morphology, A β expression, inflammatory factors, apoptotic factors, anti apoptotic factors, as well as the expression of pathway proteins and mRNA were detected.

Results: After DXP intervention, the learning and memory abilities of rats improved, the neuronal cell arrangement was more complete, the expression of A β decreased, the expression of pro-inflammatory cytokine and apoptotic factors decreased, the expression of anti apoptotic factors increased, Protein Kinase B (Akt) expression and activity significant up-regulation, and nuclear factor kappa-B (NF- κ B), p38 MAPK (p38), MAPKAPK-2 (MK2), Cyclooxygenase-2 (COX-2) protein and mRNA expression were significantly down-regulated.

Conclusion: DXP can improve the learning and cognitive abilities of AD model rats, and its mechanism of action may be related to the regulation of the Akt/NF- κ B apoptosis pathway mediated by NF- κ B interaction and the p38MAPK/MK2/COX-2 immune inflammatory dual pathway.

Keywords: Alzheimer's disease, Danzhi Xiaoyao powder, Akt/NF- κ B signaling pathway, P38MAPK/MK2/COX2 signaling pathway, neuronal apoptosis, neuronal specific inflammatory response

Introduction

Alzheimer's disease (AD) is a neurodegenerative disease characterized clinically by progressive memory, cognitive impairment, and behavioral impairment.¹ According to Lancet Public Health's research,² it is predicted that the global number of AD patients will reach 152 million by 2050, which not only poses a serious threat to human life, health and safety, but also brings serious economic burdens to families, society and countries. As is well known, the pathogenesis of Alzheimer's disease is complex, and

no drug that can completely cure its occurrence and development has been developed yet.³ Traditional Chinese Medicine Compound for the prevention and treatment of Alzheimer's disease is often reported, and its mechanism of action involves reducing the generation of A β ,⁴ the formation of neurofibrillary tangles (NFTs) due to excessive phosphorylation of tau protein,⁵ regulating small glial cells,⁶ reducing cell apoptosis,⁷ inflammatory response, oxidative stress,⁸ mitochondrial dysfunction, iron death,^{9,10} cell pyroptosis,¹¹ and other aspects. It has the characteristics of multi-target, multi mechanism regulation, significant therapeutic effect, and few side effects.^{12,13} Based on this, this article selects Okada acid, which can induce memory impairment in rats, as an inducer to establish an AD model,¹⁴ and further proposes the hypothesis of DXP treatment for AD.

DXP is derived from the Ming Dynasty book "Internal Medicine Abstract" by Xue Yi, and is a traditional Chinese medicine compound formula consisting of peony bark and gardenia, based on the classic formula Xiaoyao San (XYS) (Bupleurum, Angelica, Paeonia lactiflora, Poria cocos, Atractylodes macrocephala, and Glycyrrhiza uralensis). Previous studies on DXP have found that it can improve the activity of superoxide dismutase and choline acetyltransferase in AD model mice, reduce the activity of malondialdehyde and acetylcholinesterase, as well as the content of monoamine oxidase, enhance antioxidant and central neurotransmitter activity, and have a good preventive effect on AD.^{15,16} At the same time, YYS also has the effect of inhibiting the expression of apoptosis factor Bax and enhancing the expression of anti-apoptosis factor Bcl-2, as well as reducing the levels of inflammatory factors TNF- α , IL-1 β , and IL-6, and repairing the structural and functional damage of the hippocampus.^{17–20} In addition, modern research has shown that both Moutan Cortex and Gardenia have the effect of inhibiting apoptosis and reducing the level of inflammatory factors.^{21,22} Therefore, based on this, this article proposes the conjecture that the DXP composed of them has anti-apoptosis and anti-inflammatory mechanisms in AD.

Apoptosis is the main cause of neurodegenerative and cognitive impairment in AD.^{23,24} AKT plays a crucial role in cell survival and apoptosis, and is an indispensable anti apoptotic factor.²⁵ However, excessive accumulation of A β often inhibits the expression and phosphorylation of Akt, leading to an increase in NF- κ B activity, a large release of pro apoptotic proteins Bax (BCL2-Associated X, Bax) and caspase-3 (cysteine aspartic acid protease-3, Caspase-3), and a decrease in anti apoptotic factor Bcl-2 (B-cell lymphoma-2, Bcl-2), causing an imbalance between pro apoptotic and anti apoptotic ratios and triggering a large number of cell apoptosis.²⁶

Materials and Methods

Materials

Animals

Male Wistar rats (n=84) were purchased from the Animal Experiment Center of Gansu University of Traditional Chinese Medicine (production license: SCXK (Gan) 2020–0001) and housed at the SPF level Animal Experiment Center of Gansu University of Traditional Chinese Medicine, with a temperature of 23–25 °C and a relative humidity of 40%–60%. They were allowed to drink and eat freely. Research on animals was conducted strictly in accordance with the Laboratory Animal Protection Handbook, as well as receiving approval from the Experimental Animal Ethics Committee of Gansu University of Traditional Chinese Medicine (2021–366) for animal experiments.

Reagent

Okada Acid (Yuanye Biotechnology Co., Ltd., Shanghai, China); Donepezil Hydrochloride Tablets (Weicai Pharmaceutical Co., Ltd., Shanghai, China); IL-1 β , IL-6, TNF- α , Bcl-2, Bax and Caspase-3 kits (Enzyme-Linked Biotechnology Co., Ltd., Shanghai, China); A β Antibody(Abcam UK); P38, p-p38, MK2, COX2, Akt, p-Akt and NF- κ B antibody(Immonoway, USA); p-NF- κ B antibody (GeneTex, USA); β -Actin antibody, glyceraldehyde-3-phosphate dehydrogenase antibody (Seville Biotechnology Co., Ltd., Wuhan, China); Horseradish peroxidase (HRP)labeled goat anti-rabbit antibody, and HRP labeled goat anti-mouse antibody (Immonoway, USA); Reverse transcription, cell/tissue total RNA extraction kit (Yisheng Biotechnology Co., Ltd., Shanghai, China).

Instrument

MT-200 Morris Water Maze Video Analysis System (Taimeng Technology Co., Ltd., Chengdu, China); Type SpectraMax i3x microplate reader (Molecular Devices Co., Ltd., Shanghai, China); P100+ultra spectrophotometer (Pultton Company, USA); LightCycler96 real-time quantitative PCR instrument (Roche Company, USA); Mini P-4 vertical electrophoresis

system (Kaiyuan Xinrui Instrument Co., LTD., Beijing, China); GelView 6000Plus gel imaging system (Bolluteng Biotechnology Co., LTD., Guangzhou, China).

Drugs

DXP (Source: Internal Medicine Abstract) was purchased from the Affiliated Hospital of Gansu University of Traditional Chinese Medicine in a ratio of 2:2:2:2:1:1 based on the “13th Five Year Plan” textbook (10th edition): Chaihu, Danggui, Baishao, Fuling, Atractylodes macrocephala, Mudan Peel, Gardenia, Licorice. Soak the above decoction pieces in 10 times pure water for 30 minutes, boil for 1 hour, filter out the medicine solution, then add 10 times pure water and boil for 30 minutes, filter out the medicine solution again, concentrate the obtained medicine solution twice to a decoction with a crude drug content of 1.5 g/mL, and store it in a refrigerator at 4 °C for later use.

Method

Model Establishment, Grouping, and Treatment

Rats were randomly divided into 7 groups: normal blank group, sham operation group, model group, model+donepezil hydrochloride group, model+DXP high-dose group, model+DXP medium dose group, and model+DXP low-dose group (n=10 in each group). The AD model was replicated by bilateral hippocampal injection of Okada acid solution (100 ng) in the model group.²⁷ According to the “Pharmacological Experimental Methods” edited by Professor Xu Shuyun,²⁸ the equivalent dose ratio between humans and rats was calculated. The low, medium, and high doses of DXP were $4.38 \text{ g} \cdot \text{kg}^{-1}$, $8.77 \text{ g} \cdot \text{kg}^{-1}$, and $17.55 \text{ g} \cdot \text{kg}^{-1}$, respectively. The dose of donepezil was $5 \times 10^{-4} \text{ g} \cdot \text{kg}^{-1}$, administered orally once a day at a volume of $10 \text{ mL} \cdot \text{kg}^{-1}$. The blank group and sham surgery group were given equal volumes of physiological saline, and each group was orally administered continuously for 42 days.

Morris Water Maze Test Learning Memory Ability

The water maze pool was divided into four quadrants. The platform was placed in the center of the second quadrant (target quadrant) to inject water into the pool, so that the water surface was about 1.5 cm higher than the platform, and the water temperature was $20 \pm 2^\circ\text{C}$. Add an appropriate amount of titanium dioxide, stir evenly, and prevent rats from identifying the platform position with vision. Randomly select different quadrants, put the rats into the water with their heads facing the pool wall, and record their time to find the platform(s), that is the escape latency. If the platform was not found beyond the 60s, it was guided to reach the platform and stay for 15s. At this time, the escape latency period was recorded at the 60s. Each rat was tested once a day for 5 consecutive days. Remove the platform after the trial on day 5, the rats were put into water from the opposite side of the target quadrant, and the percentage of their moving distance in the target quadrant and the time of stagnation in the target quadrant were recorded.

Sample Collection

After the Morris water maze test, the rats were anesthetized by intraperitoneal injection of 3% pentobarbital sodium solution (0.35mL/100g), followed by execution by cervical dislocation. The brain was taken by craniotomy, one part was stored in 4% paraformaldehyde solution for HE staining and immunohistochemical analysis, and the other was quickly stripped off from the hippocampus on ice and stored in the -80°C refrigerator for ELISA, WB, and RT-PCR detection.

Hematoxylin-Eosin (HE) Staining

The brain tissue was fixed in 4% paraformaldehyde solution for 8 h, paraffin-embedded sections were made. Xylene and gradient alcohol were used to dewax to water, hematoxylin staining for 5 min, 1% hydrochloric acid ethanol differentiation, anti-blue, eosin staining for 3 min, dehydration, film sealing, and microscopic observation of hippocampal cell morphology and photography.

Immunohistochemical and Quantitative Analysis of A β in Hippocampus Expression

The brain tissues were embedded, sectioned, and dewaxed. Citrate buffer antigen were repaired, boiled 3 min, 37°C warm tank serum was closed 30 min, add A β primary antibody (1:200), 4°C overnight, PBS for 5 min, add secondary antibody, 37°C warm box incubation 30 min, dripping with DAB, color solution, hematoxylin redye, dehydration, sealing, observed and photographed. The positive expression in each group was counted with Image-ProPlus 6.0 image

processing software using statistics of integrated optical density (IOD). Mean optical density equals the sum of IOD divided by the area.

Detection of Pro-Inflammatory Factors and Apoptosis Factors in Hippocampus by Enzyme-Linked Immunosorbent Assay (ELISA)

Hippocampal tissue supernatant was prepared, and operated strictly according to the kit instructions, and the optical density value of each well was determined at 450 nm to calculate the contents of pro-inflammatory factors IL-1 β , IL-6, TNF- α , and apoptotic factors Bcl-2, Bax, and Caspase-3.

The Expression of p38, p-p38, MK2, COX-2, Akt, p-Akt, NF- κ B, and p-NF- κ B Was Detected by Western Blotting (WB)

Hippocampal tissue supernatant was extracted, and after the protein concentration was determined by BCA, 10%SDS-PGE gel was configured, and a 35 μ g sample was taken to electrophoresis (80/120V), the goal protein was transferred to the PVDF membrane (100V, 75 min). Subsequently, 5% skim milk or 5%BSA blocking solution was blocked for 2 h, adding diluted (1:1000) primary antibody p38, p-p38, MK2, COX-2, Akt, p-Akt, NF- κ B and p-NF- κ B, 4°C refrigerator overnight. The next day, the shaker was gently shaken for 30 min and washed three times in PBST for 10 min each, then diluted (1:10,000) of secondary antibody GAPDH and β -actin were incubated for 90 min, the previous step of washing step was repeated, exposed to the gel imager, and the gray values were analyzed by Image J software.

The Expression of p38, MK2, and COX-2 mRNA Was Detected by Real-Time Fluorescence Quantitative PCR

By weighing the hippocampal tissue, adding the L B Buffer's, homogenate, and centrifugation at 12000r/min 5 min, the supernatant was transferred to enzyme-free centrifuge tubes. Strictly following the RNA extraction kit instructions, after concentration detection using a spectrophotometer, the RNA was reverse transcribed to cDNA according to the reverse transcription kit instructions. Amplification was performed using a two-step method. The program settings are as follows: 95°C pre-denature and 5 min, 95°C denaturation for 10s, and 60°C annealing/extension for the 30s. Fluorescent signals were collected after 40 cycles. GAPDH was used as an internal parameter, and the relative expression level of p38, MK2, and COX-2 mRNA was calculated with the $2^{-\Delta\Delta C_t}$ method. The primers were synthesized by Beijing Biomed Biotechnology Co., Ltd, and the sequences are shown in Table 1.

Statistical Analysis

All data collected in the study are presented as mean \pm SEM. One way ANOVA was used for inter group comparison, and the least significant difference (LSD) method was used for homogeneity of variance. Dunnett's method was used for heterogeneity, and Prism 10.0 software was used to analyze the results. $P < 0.05$ was considered statistically significant. Perform principal component analysis and partial least squares clustering analysis on FNIRs using SIMCA 14.1 software.

Table 1 Primer Sequence

Primer	Sequence (5'→3')	Length b/p
GAPDH	Sense strand: GACATGCCGCCTGGAGAAAC Antisense strand: AGCCCAGGATGCCCTTTAGT	92
p38	Sense strand: CAGTCCATCATTACGC Antisense strand: CATTACAGCGAGGTTG	301
MK2	Sense strand: GGAAGTGCTTGCTGATTG Antisense strand: GAGTTGTGACTGGTGGTTTC	265
COX-2	Sense strand: GGAGTCTGGAACATTGTG Antisense strand: TAGGAGAGGTTGGAGAAAG	152

Results

DXP Improves Learning and Memory Ability of AD Model Rats

Compared with the blank control group, the activity trajectory of the model group was significantly prolonged (Figures 1a-e), and the time to first reach the platform and the escape latency were significantly prolonged ($P < 0.01$) (Figures 2 and 3), and the percentage of target quadrant movement distance and retention time were significantly shortened in the model group ($P < 0.01$) (Figures 4 and 5). There was no significant change in the sham operation group; Compared with the model group, the activity tracking of the drug administration group was significantly shortened (Figure 1), and the first arrival time and escape latency of the drug group were shortened ($P < 0.01$, $P < 0.05$) (Figures 2 and 3), the percentage of target quadrant movement distance was increased, and the retention time was prolonged ($P < 0.05$, $P < 0.01$) (Figures 4 and 5).

DXP Relieves Neuronal Damage in the CA1 Region of the Hippocampus

As shown in Figures 6a-e, compared with the control group, the cells in the model group were arranged disorderly, with deep staining of karyopyknosis and vacuolar structure, and a large number of apoptotic cells, while no significant changes were observed in the sham operation group. Compared with the model group, the neurons in each treatment group were arranged neatly, with clear and plump cell bodies, and apoptotic cells were reduced.

DXP Decreases the Expression of A β in the Hippocampus

Compared with the control group, the expression of A β was significantly increased in the model group (Figures 7a-e), and there was no significant change in the sham group ($P < 0.01$) (Figure 8). Compared with the model group, the expression of A β was decreased in each treatment group ($P < 0.01$, $P < 0.05$) (Figure 8).

DXP Reduces the Contents of Pro-Inflammatory Factors, IL-1 β , IL-6, and TNF- α in the Hippocampal

Compared with the control group, the contents of IL-1 β , IL-6, and TNF- α in the model group hippocampus were significantly increased, and there was no significant change in the sham group ($P < 0.01$) (Figures 9–11). Compared with the model group, the contents of IL-1 β , IL-6, and TNF- α were significantly reduced in each treatment group ($P < 0.01$) (Figures 9–11).

DXP Reduces the Content of Apoptotic Factors, Bcl-2, Bax, and Caspase-3 in the Hippocampal

Compared with the control group, the contents of Bcl-2 were significantly reduced ($P < 0.01$) (Figure 12), the contents of Bax and Caspase-3 were significantly higher ($P < 0.01$) (Figures 13 and 14), the Bcl-2/Bax ratio was significantly decreased ($P < 0.01$) (Figure 15) in model group and there was no significant change in the sham group. Compared with the model group, the contents of Bcl-2 was significantly higher ($P < 0.01$) (Figure 12), Bax and Caspase-3 was decreased ($P < 0.01$, $P < 0.05$) (Figures 13 and 14), and the Bcl-2/Bax ratio was significantly increased in each treatment group ($P < 0.01$) (Figure 15).

DXP Elevates Akt Activity and Suppresses NF- κ B Activity in the Hippocampal

Compared with the control group, the expression of Akt and p-Akt were decreased significantly, the expression of NF- κ B and p-NF- κ B were significantly increased in the model group ($P < 0.01$) (Figures 16–20), and there was no significant change in the sham group. Compared with the model group, the expression of Akt and p-Akt was increased and the NF- κ B, and p-NF- κ B expression were decreased in each treatment group ($P < 0.01$, $P < 0.05$) (Figures 16–20).

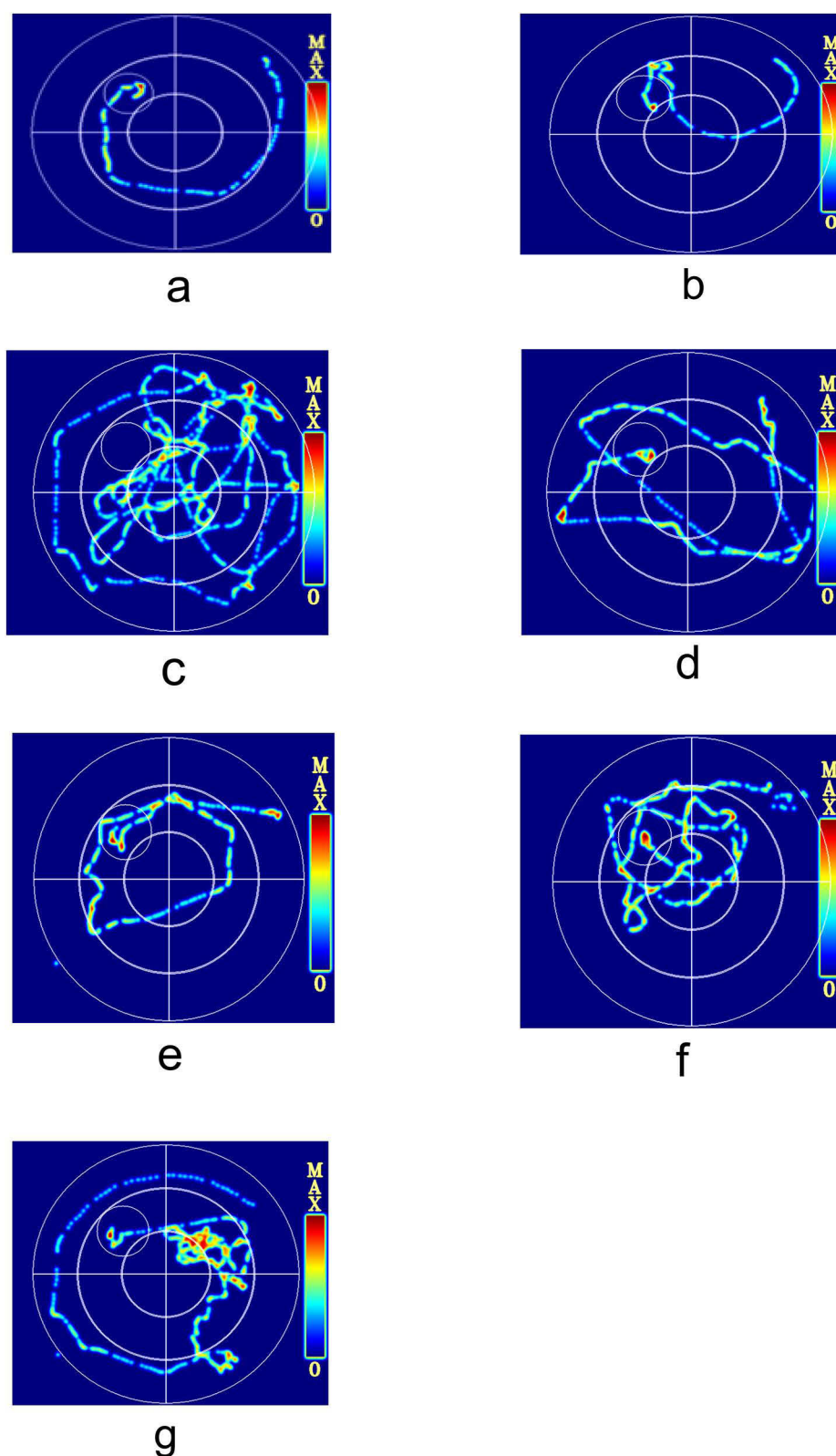


Figure 1 (a) Morris water maze trajectory diagram of Blank control group AD model rats. (b) Morris water maze trajectory diagram of Sham operation group AD model rats. (c) Morris water maze trajectory diagram of Model group AD model rats. (d) Morris water maze trajectory diagram of Model+Donepezil hydrochloride group AD model rats. (e) Morris water maze trajectory diagram of Model+DXP high-dose group AD model rats. (f) Morris water maze trajectory diagram of Model+DXP medium-dose group AD model rats. (g) Morris water maze trajectory diagram of Model+DXP low-dose group AD model rats.

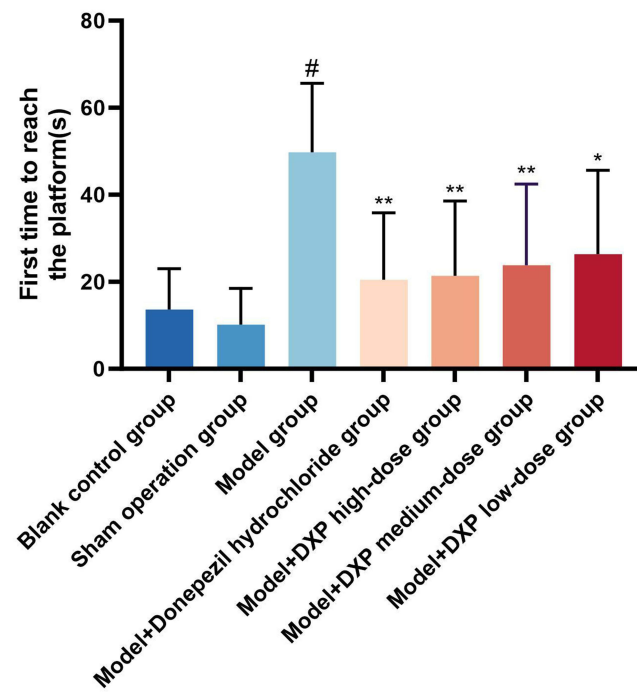


Figure 2 The first arrival time of AD model rats in different groups at the platform(s).

Notes: # $P < 0.01$ vs Blank control group; * $P < 0.05$, ** $P < 0.01$ vs Model group.

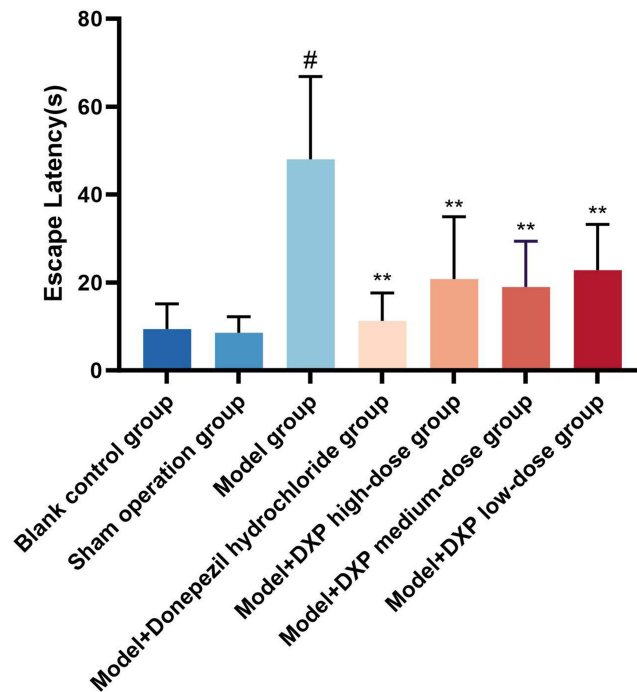


Figure 3 Avoidance latency period of AD model rats in different groups.

Notes: # $P < 0.01$ vs Blank control group; * $P < 0.05$, ** $P < 0.01$ vs Model group.

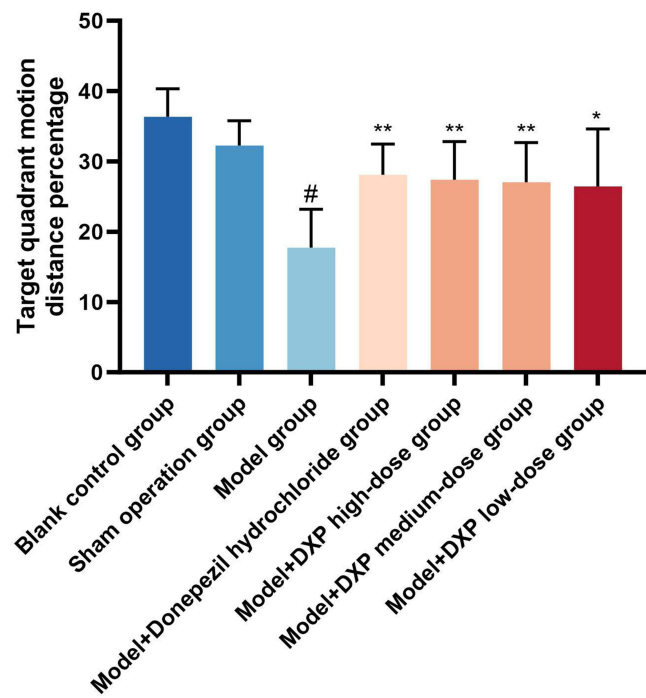


Figure 4 Percentage of target quadrant motion distance in AD model rats of different groups.
Notes: # $P<0.01$ vs Blank control group; * $P<0.05$, ** $P<0.01$ vs Model group.

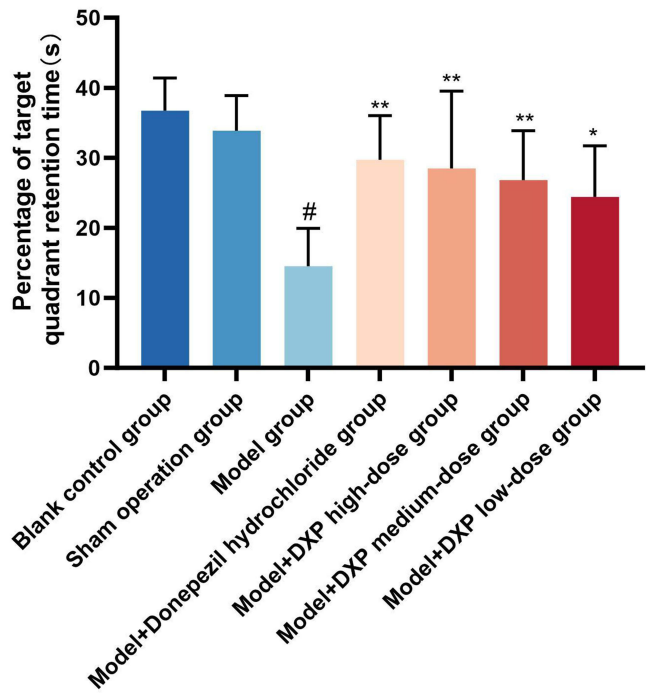


Figure 5 Percentage of target quadrant retention time in AD model rats of different groups.
Notes: # $P<0.01$ vs Blank control group; * $P<0.05$, ** $P<0.01$ vs Model group.

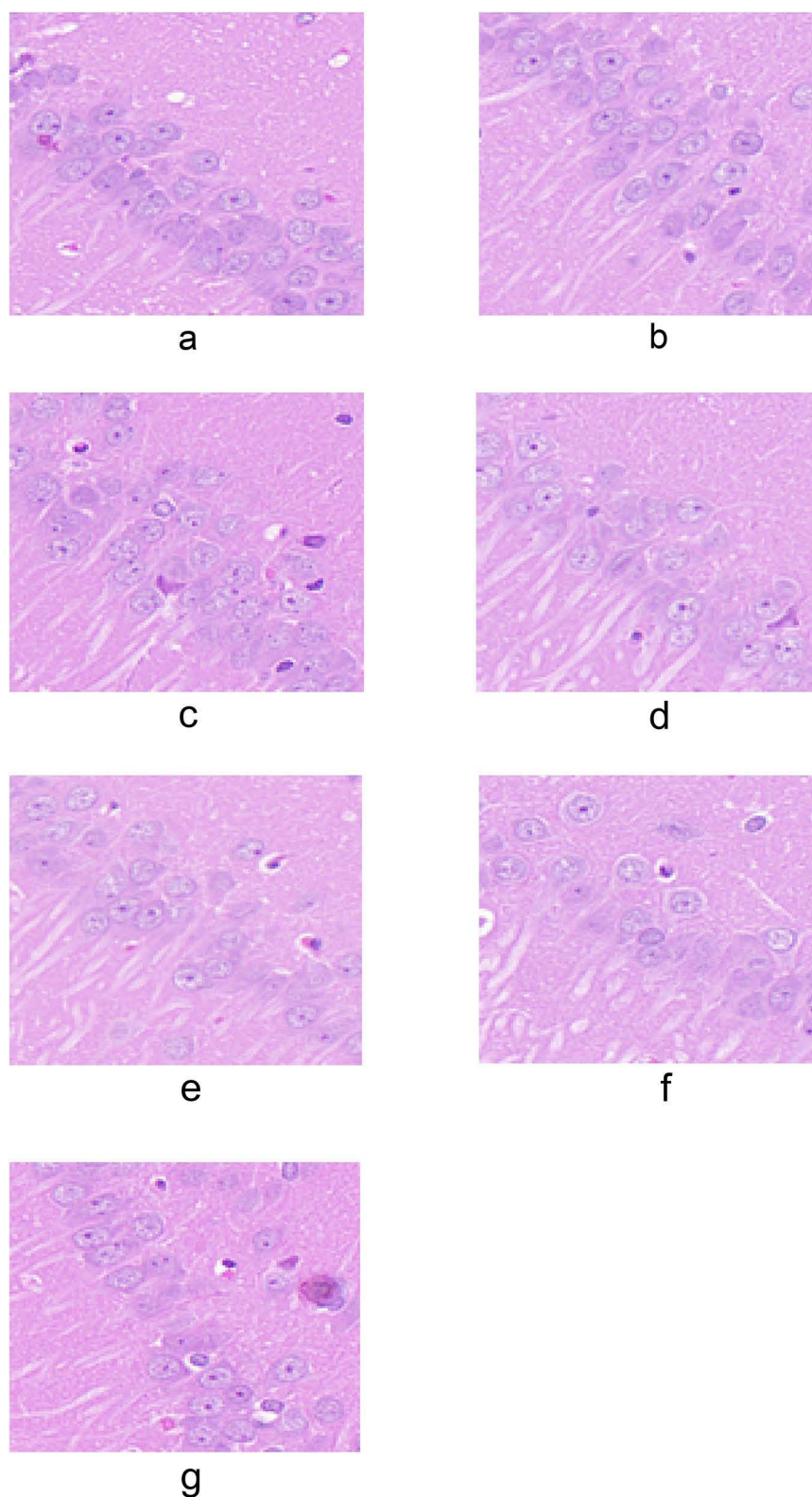


Figure 6 (a) Neuronal damage in the hippocampal CA1 region of the Blank control group. (b) Neuronal damage in the hippocampal CA1 region of the Sham operation group. (c) Neuronal damage in the hippocampal CA1 region of the Model group. (d) Neuronal damage in the hippocampal CA1 region of the Model+Donepezil hydrochloride group. (e) Neuronal damage in the hippocampal CA1 region of the Model+DXP high-dose group. (f) Neuronal damage in the hippocampal CA1 region of the Model+DXP medium-dose group. (g) Neuronal damage in the hippocampal CA1 region of the Model+DXP low-dose group.

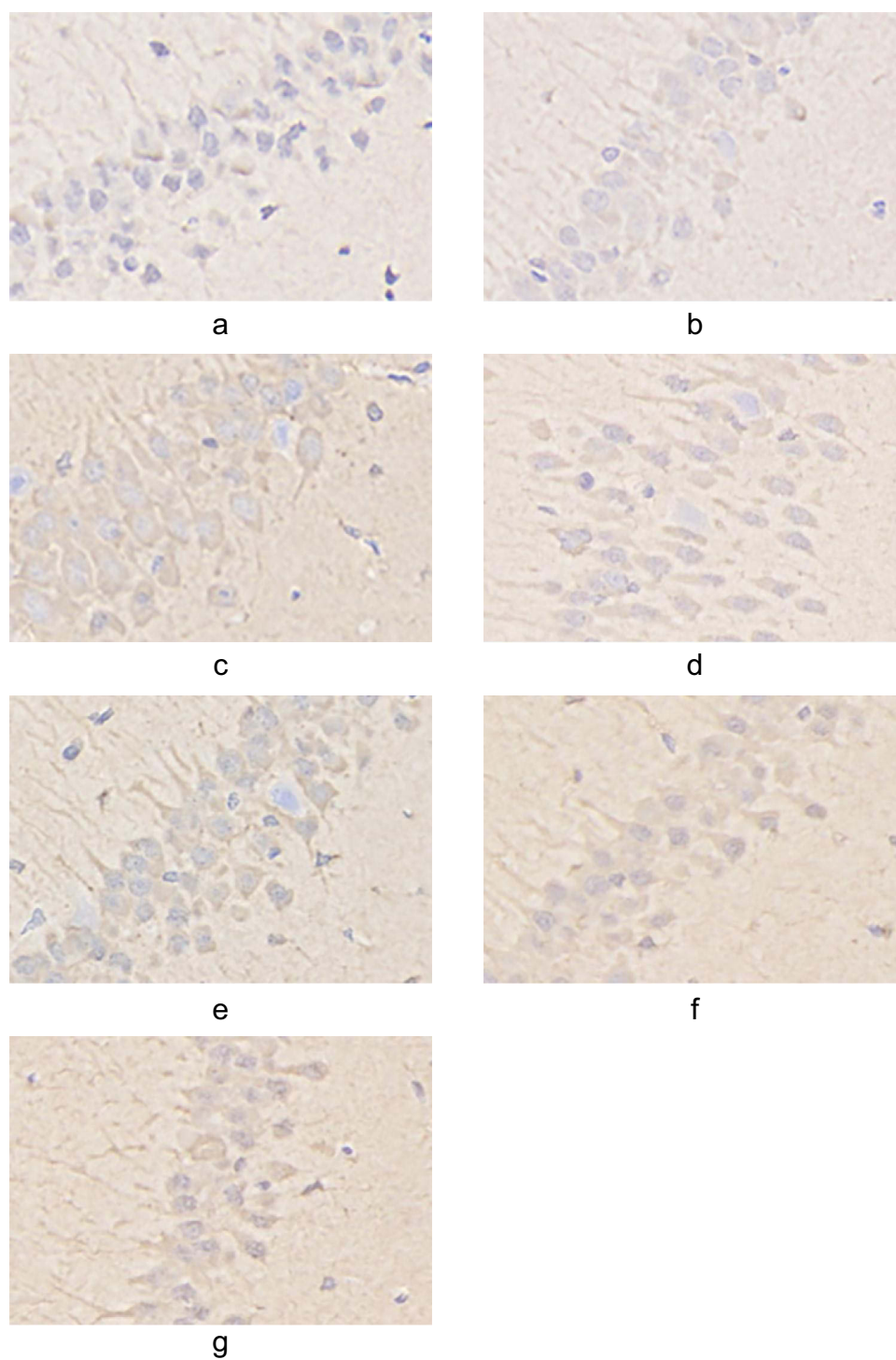


Figure 7 (a) Expression of A β in the Blank control group hippocampus. (b) Expression of A β in the Sham operation group hippocampus. (c) Expression of A β in the Model group hippocampus. (d) Expression of A β in the Model+Donepezil hydrochloride group hippocampus. (e) Expression of A β in the the Model+DXP high-dose group hippocampus. (f) Expression of A β in the the Model+DXP medium-dose group hippocampus. (g) Expression of A β in the the Model+DXP low-dose group hippocampus.

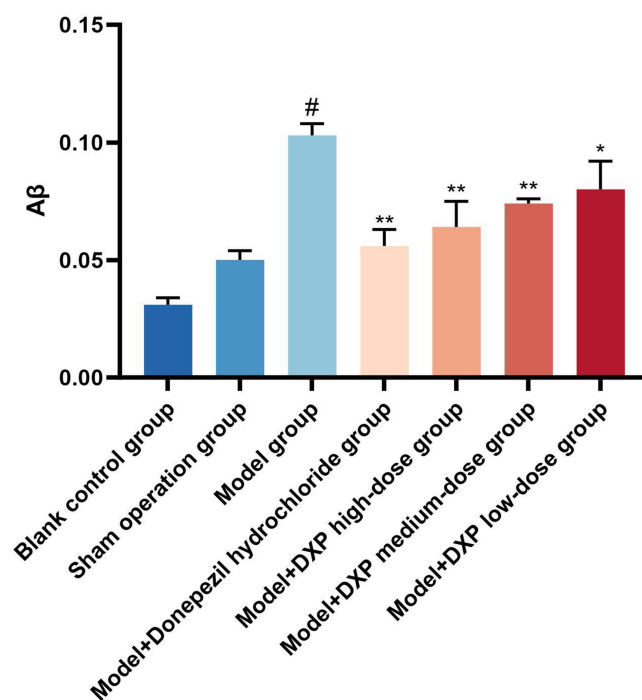


Figure 8 Expression of A β in AD model rats in different groups.

Notes: # P <0.01 vs Blank control group; * P <0.05, ** P <0.01 vs Model group.

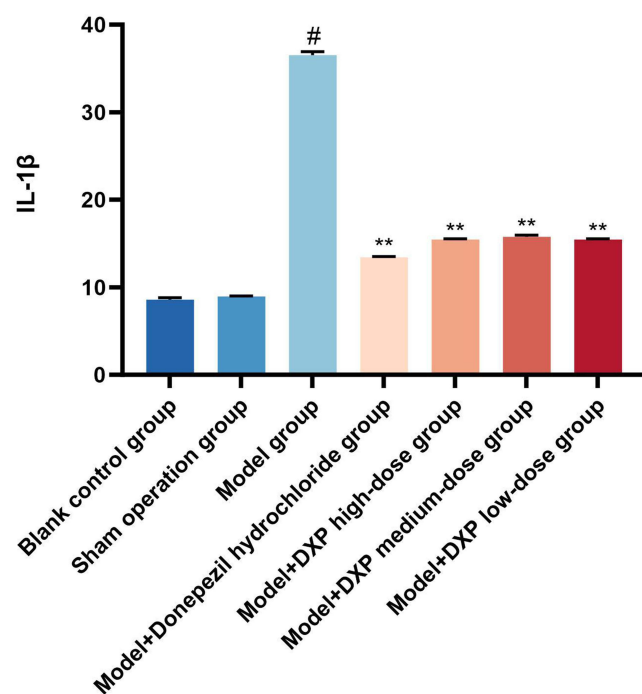


Figure 9 Expression of IL-1 β in AD model rats in different groups.

Notes: # P <0.01 vs Blank control group; * P <0.05, ** P <0.01 vs Model group.

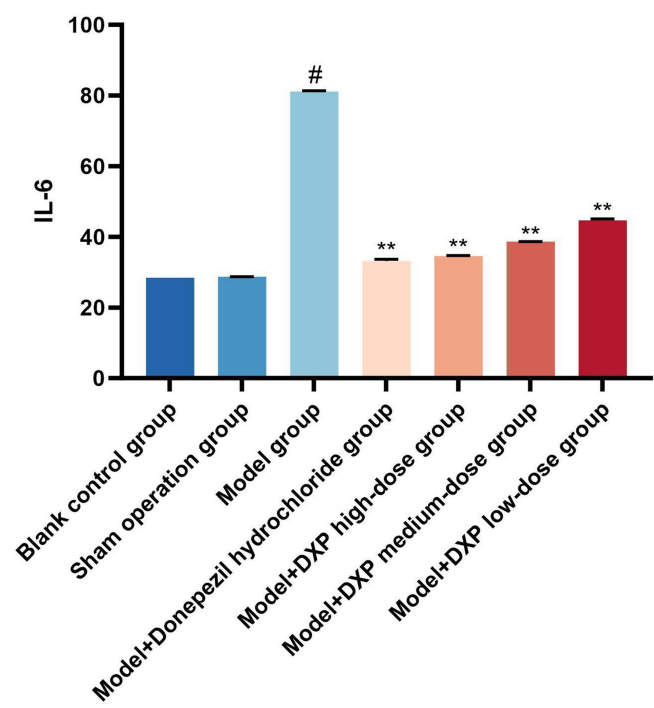


Figure 10 Expression of IL-6 in AD model rats in different groups.
Notes: #*P*<0.01 vs Blank control group; **P*<0.05, ***P*<0.01 vs Model group.

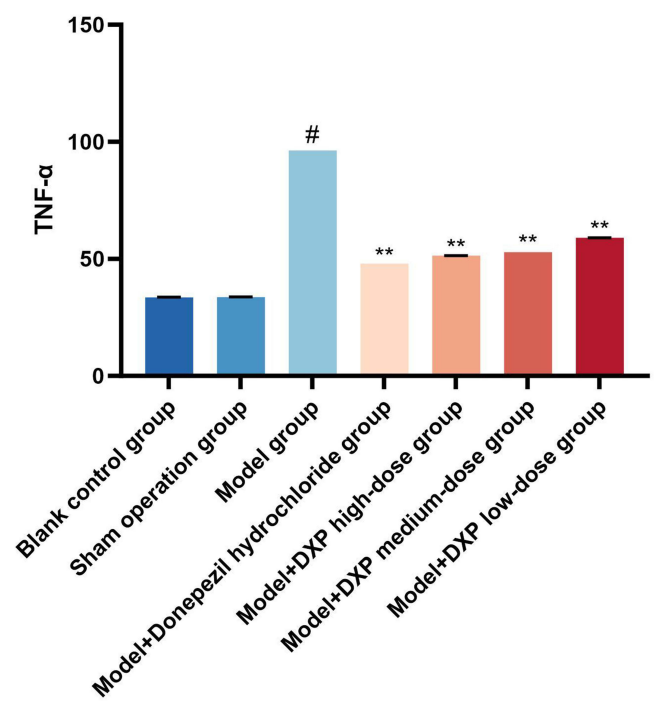


Figure 11 Expression of TNF-α in AD model rats in different groups.
Notes: #*P*<0.01 vs Blank control group; **P*<0.05, ***P*<0.01 vs Model group.

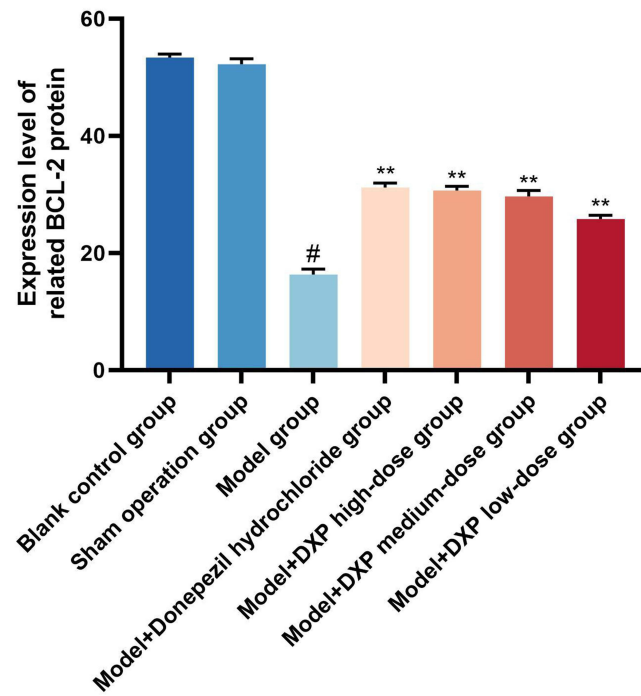


Figure 12 Expression of BCL-2 in AD model rats in different groups.
Notes: [#] $P < 0.01$ vs Blank control group; ^{*} $P < 0.05$, ^{**} $P < 0.01$ vs Model group.

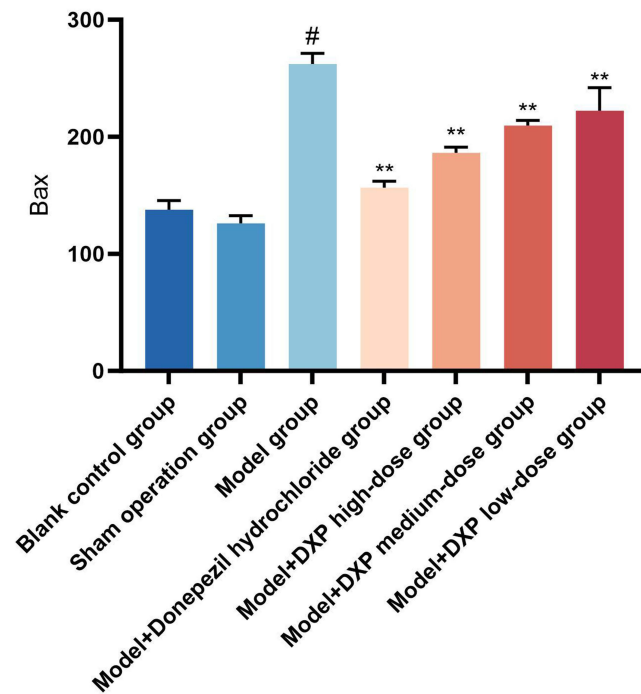


Figure 13 Expression of Bax in AD model rats in different groups.
Notes: [#] $P < 0.01$ vs Blank control group; ^{*} $P < 0.05$, ^{**} $P < 0.01$ vs Model group.

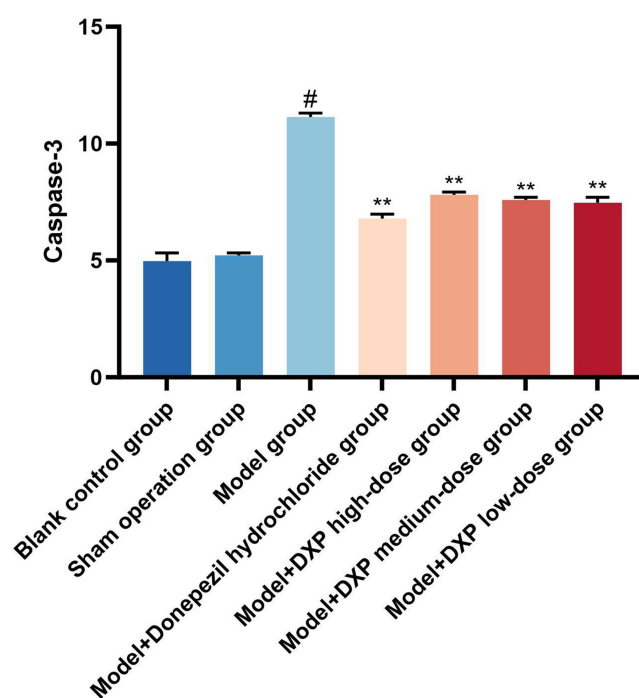


Figure 14 Expression of Caspase-3 in AD model rats in different groups.
Notes: # $P < 0.01$ vs Blank control group; * $P < 0.05$, ** $P < 0.01$ vs Model group.

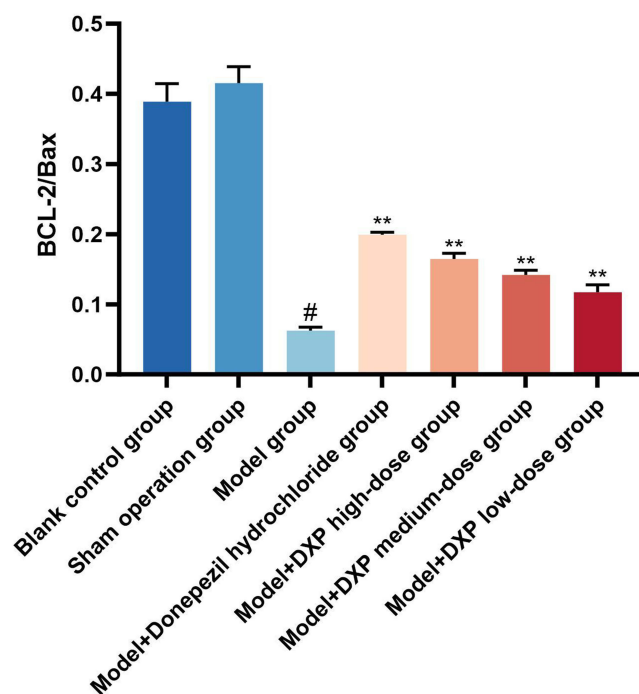


Figure 15 Expression of BCL-2/Bax in AD model rats in different groups.
Notes: # $P < 0.01$ vs Blank control group; * $P < 0.05$, ** $P < 0.01$ vs Model group.

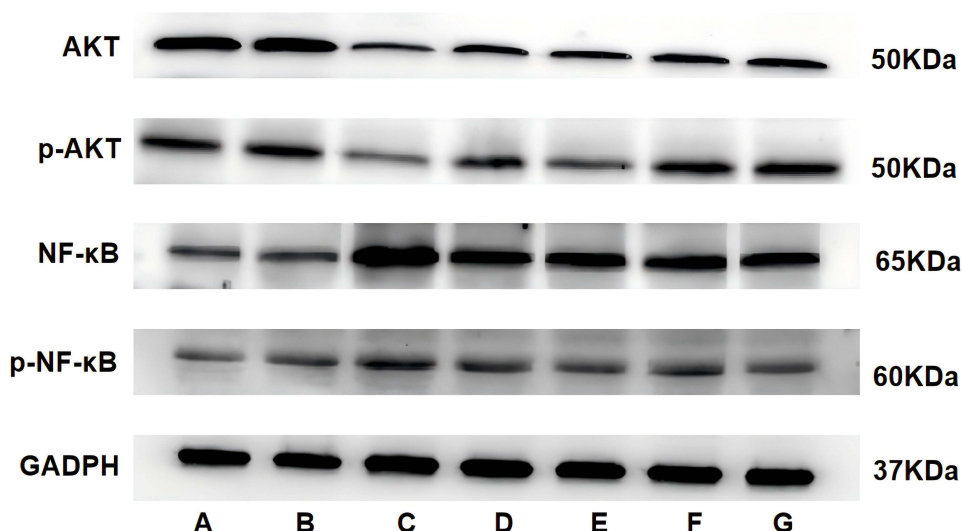


Figure 16 The expression levels of AKT, p-AKT, NF-κB and p-NF-κB in the hippocampus.

Notes: (A) Blank control group; (B) Sham operation group; (C) Model group; (D) Model+Donepezil hydrochloride group; (E) Model+DXP high-dose group; (F) Model+DXP medium-dose group; (G) Model+DXP low-dose group.

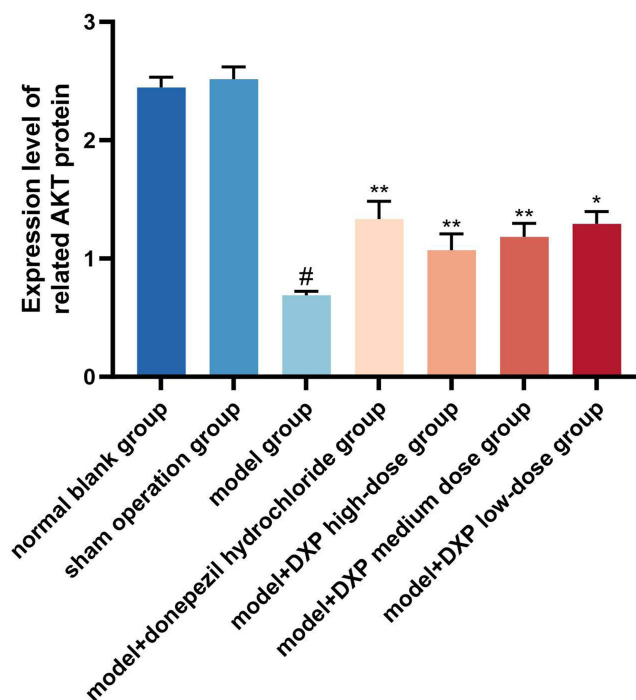


Figure 17 Expression level of related AKT protein.

Notes: # $P < 0.01$ vs Blank control group; * $P < 0.05$, ** $P < 0.01$ vs Model group.

DXP Reduces the Expression Levels of p38, p-p38, MK2, and COX-2 in the Hippocampus

Compared with the control group, the expression levels of p38, p-p38, MK2, and COX-2 were significantly increased in the model group ($P < 0.01$) (Figures 21–25), and there was no significant change in the sham group. Compared with the model group, the expression levels of p38, p-p38, MK2, and COX-2 were reduced in each treatment group ($P < 0.01$, $P < 0.05$) (Figures 21–25).

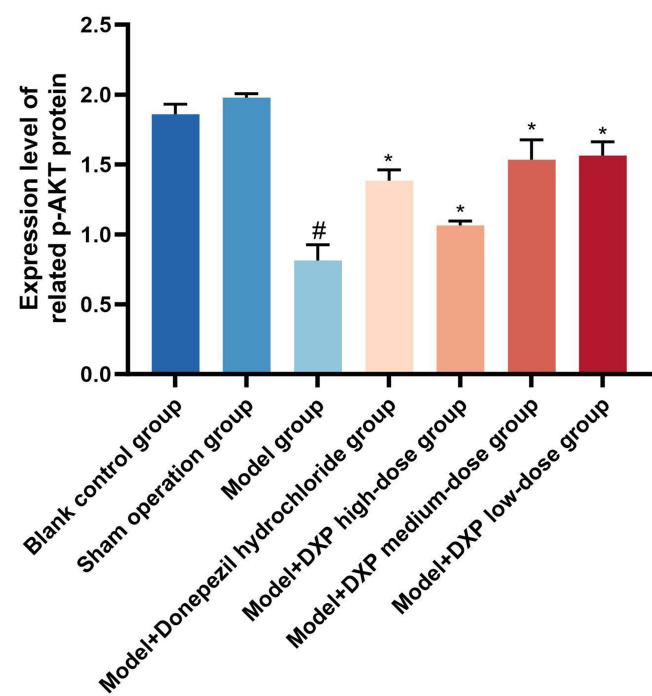


Figure 18 Expression level of related p-AKT protein.
Notes: [#] $P<0.01$ vs Blank control group; ^{*} $P<0.05$, ^{**} $P<0.01$ vs Model group.

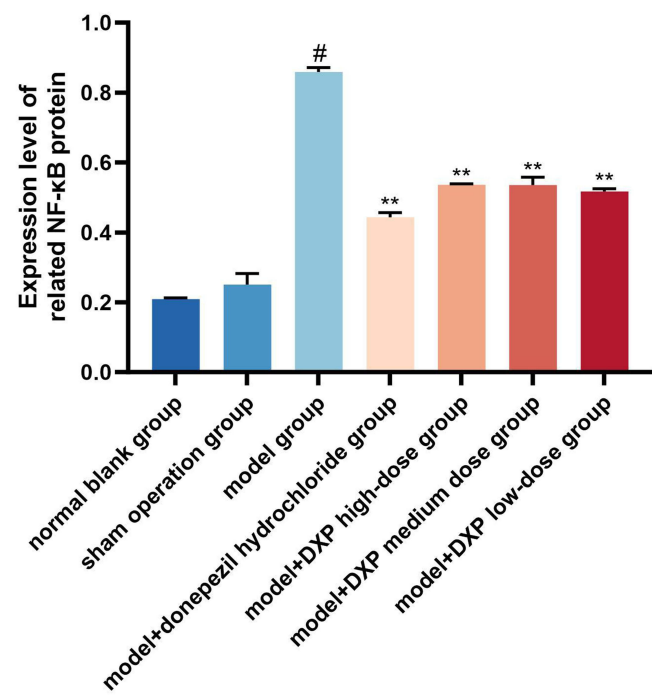


Figure 19 Expression level of related NF-κB protein.
Notes: [#] $P<0.01$ vs Blank control group; ^{*} $P<0.05$, ^{**} $P<0.01$ vs Model group.

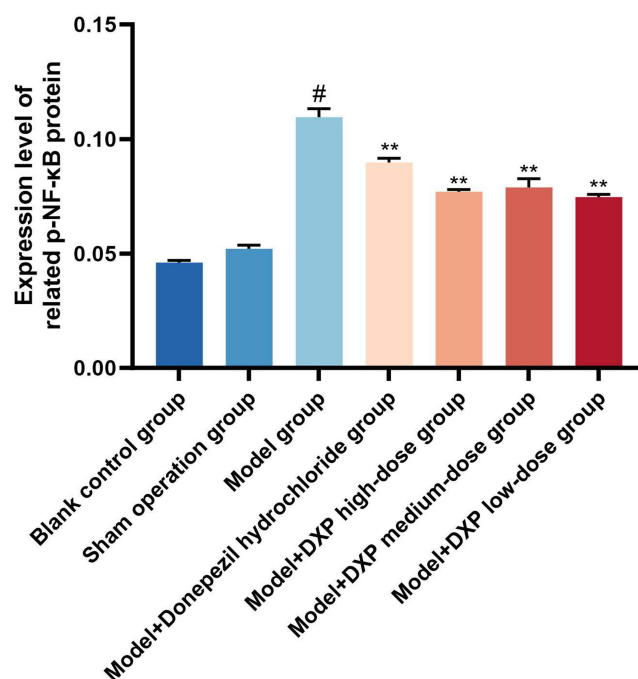


Figure 20 Expression level of related p-NF-κB protein.

Notes: [#] $P < 0.01$ vs Blank control group; ^{*} $P < 0.05$, ^{**} $P < 0.01$ vs Model group.

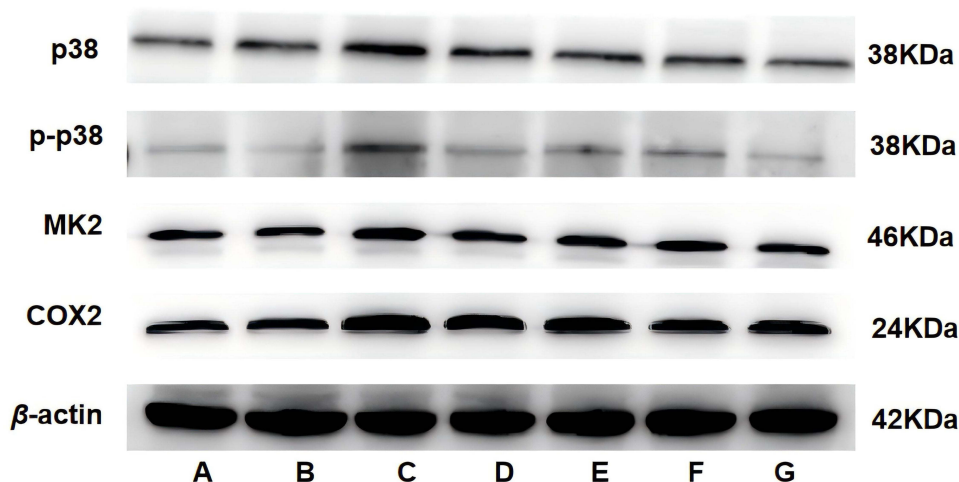


Figure 21 The expression levels of p38, p-p38, MK2, and COX-2 in the hippocampus.

Notes: (A) Blank control group; (B) Sham operation group; (C) Model group; (D) Model+Donepezil hydrochloride group; (E) Model+DXP high-dose group; (F) Model+DXP medium-dose group; (G) Model+DXP low-dose group.

DXP Reduces the Gene Expression of p38, MK2, and COX-2 mRNA in the Hippocampus

Compared with the control group, the expression of p38, MK2, and COX-2 mRNA were significantly increased ($P < 0.01$) (Figures 26–28), and there was no significant change in the sham group. Compared with the model group, the expression of p38, MK2, and COX-2 mRNA were significantly decreased in each treatment group ($P < 0.01$) (Figures 26–28).

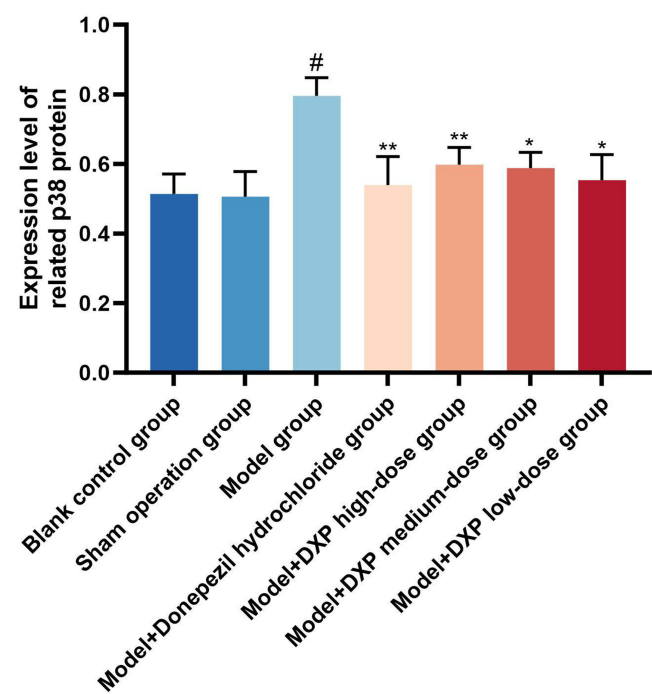


Figure 22 Expression level of related p38 protein.
Notes: # $P<0.01$ vs Blank control group; * $P<0.05$, ** $P<0.01$ vs Model group.

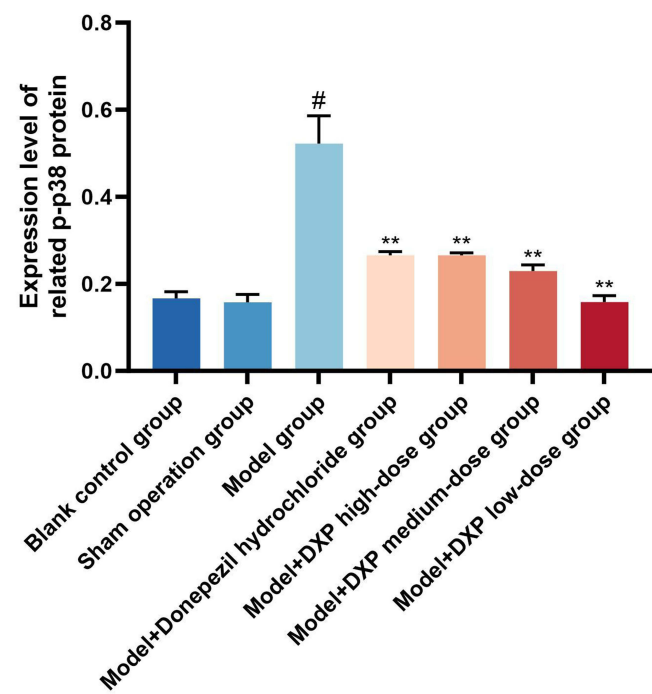


Figure 23 Expression level of related p-p38 protein.
Notes: # $P<0.01$ vs Blank control group; * $P<0.05$, ** $P<0.01$ vs Model group.

Discussion

AD belongs to the category of “dementia” in traditional Chinese medicine. With the increasing aging of the world population, AD has become a health problem that troubles the physical and mental health of middle-aged and elderly people. Therefore, based on traditional Chinese medicine theory and clinical practice, the research group proposes the use

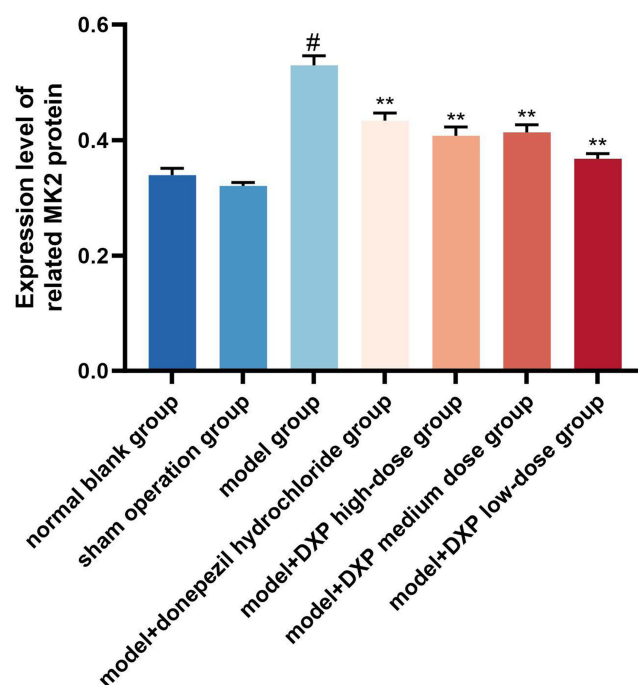


Figure 24 Expression level of related MK2 protein.

Notes: [#] $P < 0.01$ vs Blank control group; ^{*} $P < 0.05$, ^{**} $P < 0.01$ vs Model group.

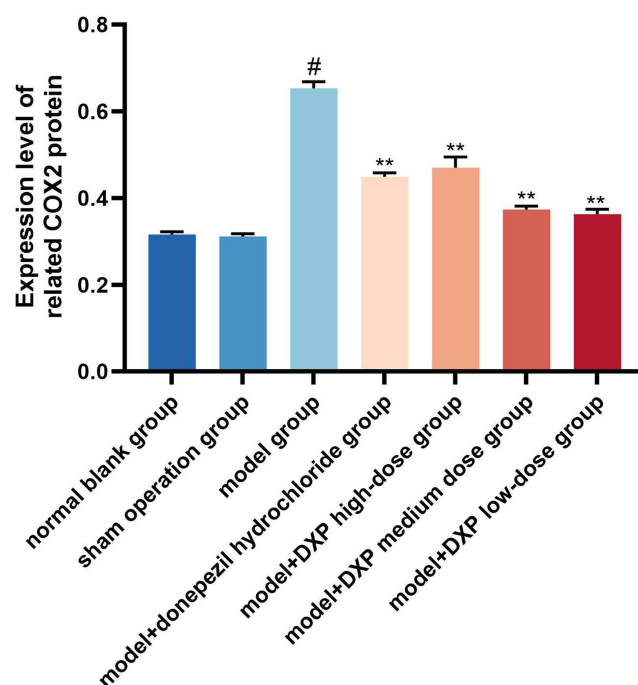


Figure 25 Expression level of related COX2 protein.

Notes: [#] $P < 0.01$ vs Blank control group; ^{*} $P < 0.05$, ^{**} $P < 0.01$ vs Model group.

of DXP, a traditional Chinese medicine compound composed of peony bark and gardenia, in the treatment of AD. Previous experiments have shown that DXP has the effect of reducing the levels of inflammatory factors TNF- α and IL-6 and alleviating neuronal cell apoptosis in the treatment of depression.^{29,30}

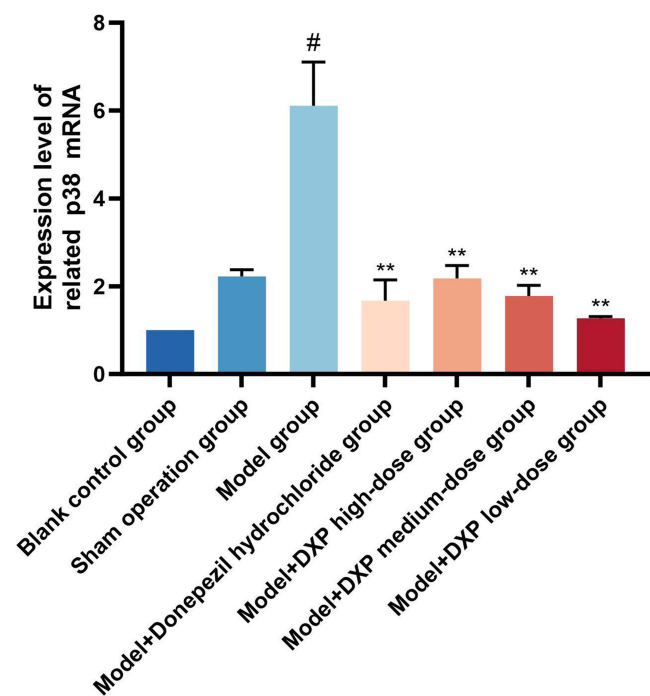


Figure 26 Expression level of related p38 mRNA.
Notes: [#] $P<0.01$ vs Blank control group; ^{*} $P<0.05$, ^{**} $P<0.01$ vs Model group.

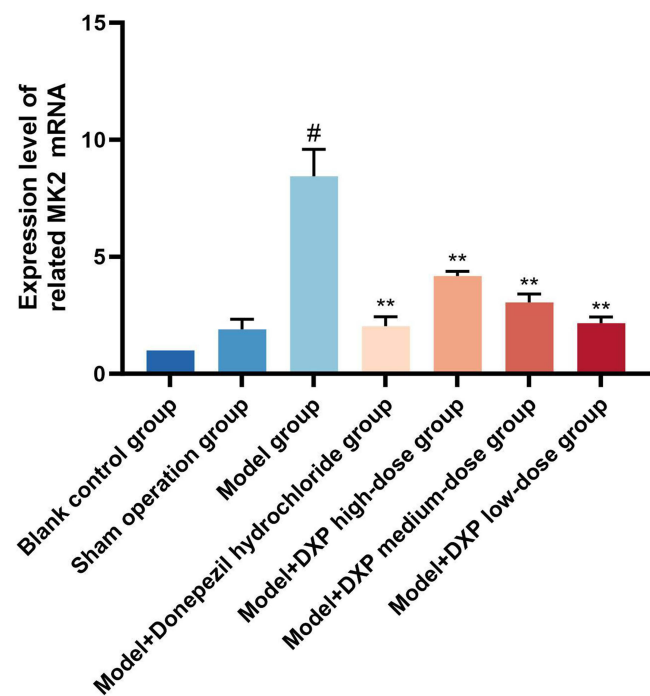


Figure 27 Expression level of related MK2 mRNA.
Notes: [#] $P<0.01$ vs Blank control group; ^{*} $P<0.05$, ^{**} $P<0.01$ vs Model group.

AKT, as an important factor for cell survival and apoptosis, its abnormal expression can trigger various diseases such as neurological disorders.^{31–33} Jaiswal et al³⁴ confirmed that inhibiting AKT leads to neuronal cell apoptosis, while activating the Akt pathway can significantly improve apoptosis. It has also been confirmed in 5XFAD

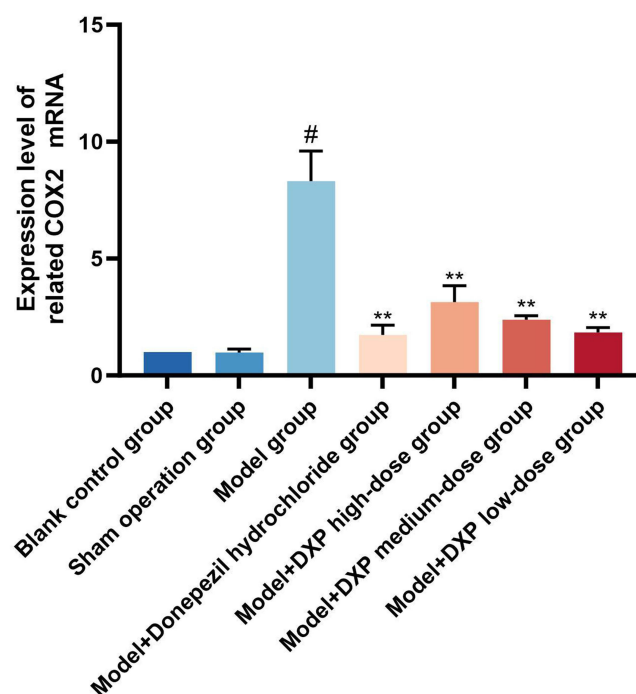


Figure 28 Expression level of related COX2 mRNA.

Notes: # $P < 0.01$ vs Blank control group; * $P < 0.05$, ** $P < 0.01$ vs Model group.

transgenic mice that the use of AKT activators can rescue memory impairment and abnormal synaptic plasticity caused by A β .³⁵ Meanwhile, studies³⁶ have also found that AKT participates in cell apoptosis by regulating the activity of downstream factor NF- κ B, thereby modulating the expression of Bax, Caspase-3, and Bcl-2.^{37,38} In addition, NF- κ B not only participates in cell apoptosis response, but also serves as a key protein regulating cellular inflammatory response, participating in AD neuroinflammatory response.³⁹ Research has found that when NF- κ B activity increases, the expression level of p38 protein also increases, accelerating NF- κ B activation, releasing a large amount of inflammatory factors, and inducing neuroinflammatory reactions.²⁴ Among them, the activation of MK2, a direct downstream substrate of p38, plays an indispensable role. On the one hand, MK2 prevented the inhibitory effect of mitogen and stress activated protein kinase 1 on NF- κ B activity, increased the transcriptional activity of NF- κ B, and elevated the levels of pro-inflammatory cytokines TNF- α , IL-1 β , IL-6, and COX-2.⁴⁰ On the other hand, MK2 exacerbates the inflammatory response by directly regulating downstream levels of TNF- α , IL-1 β , IL-6, and COX-2.²⁸ In experiments using MK2 inhibitors to intervene in inflammatory diseases, a decrease in pro-inflammatory cytokine levels was also found, indicating that the p38-MK2 signaling axis is a key link in regulating inflammatory responses.⁴¹ Meanwhile, studies have also shown that p38 is directly activated by A β and releases inflammatory factors through the p38-MK2 signaling axis, participating in the neuroinflammatory response of Alzheimer's disease.^{25,27} Therefore, DXP was selected as the intervention drug in this study, with donepezil hydrochloride tablets, which have inhibitory effects on apoptosis and pro-inflammatory cytokine release, as the positive control drug.^{42,43} Selecting apoptotic and inflammatory markers such as Bax, Caspase-3, Bcl-2, IL-1 β , IL-6, TNF- α , AKT, NF- κ B, p38, MK2, COX-2, to observe the effects and regulatory effects of acupuncture DXP on hippocampal apoptosis and inflammatory damage in AD model rats. The aim is to reveal the neural cell molecular mechanism of DXP treatment for AD through the dual pathways of NF- κ B mediated cell apoptosis and immune inflammatory response. This experiment used bilateral hippocampal injection of Okadaic acid to replicate the AD rat model. After modeling, the rats showed clinical symptoms such as liking quietness, preferring solitude, decreased flexibility, and being prone to restlessness when facing unfamiliar environments. The Morris water maze test is the gold standard for assessing spatial learning and memory, which can detect the learning and memory abilities of

experimental animals towards spatial position and orientation (spatial localization).⁴⁴ The Morris water maze test was used in this experiment to evaluate the success of the AD model and the changes in learning and memory of rats in each group after administration. The results showed that after DXP intervention, the learning and memory abilities of rats were improved, manifested as shortened activity trajectories, shortened first arrival time and escape latency, increased percentage of target quadrant movement distance, and prolonged retention time; Hippocampal neurons are arranged neatly, with clear and plump cell bodies, reduced apoptotic cells, and decreased expression of A β ; At the same time, AKT protein expression increased, NF- κ B protein expression decreased, p38, MK2, COX-2 protein and mRNA expression decreased, anti apoptotic factor Bcl-2 content significantly increased, apoptotic Bax and Caspase-3 content decreased, and inflammatory factors TNF- α , IL-1 β , IL-6 levels significantly decreased. The above results indicate that DXP can regulate the AKT/NF- κ B and p38MAPK/MK2/COX-2 pathways mediated by NF- κ B, reduce the expression of A β , increase the content of anti apoptotic factor Bcl-2, downregulate the content of apoptotic Bax and Caspase-3, and reduce the levels of inflammatory factors TNF- α , IL-1 β and IL-6, thereby alleviating neuroinflammatory response and cell apoptosis in Haima. The hippocampus is a brain region closely related to cognitive and memory functions, and improving learning and memory dysfunction in rats can be achieved by reducing cell apoptosis and inflammatory reactions in the hippocampus. In addition, DXP may also improve cognitive impairment in AD model rats by regulating neural plasticity in the hippocampus, restoring normal neuronal function. Based on this, it is speculated that the possible mechanism by which DXP improves cognitive impairment in AD model rats is related to regulating the NF- κ B-mediated AKT/NF- κ B and p38MAPK/MK2/COX-2 pathways, reducing A β production, inhibiting cell apoptosis, and neuroinflammatory responses. However, there are certain shortcomings in this study. The pathogenesis of AD is complex and variable. Therefore, in the next step of the experiment, a blocking agent group can be set up to more comprehensively explain the regulation of NF- κ B mediated AKT/NF- κ B and p38MAPK/MK2/COX-2 pathways by DXP to reduce cell apoptosis and inflammatory response in the treatment of AD. At the same time, a more comprehensive experimental plan can be proposed to explore the specific mechanism of DXP in the treatment of AD.

Ethics Approval

This experiment has been approved by the Experimental Animal Ethics Committee of Gansu University of Traditional Chinese Medicine (2021-366).

Consent for Publication

All authors have given final approval of the version and agreed with the publication of this study here.

Author Contributions

All authors made a significant contribution to the work reported, whether that is in the conception, study design, execution, acquisition of data, analysis and interpretation, or in all these areas; took part in drafting, revising or critically reviewing the article; gave final approval of the version to be published; have agreed on the journal to which the article has been submitted; and agree to be accountable for all aspects of the work. This research was partially supported by the National Natural Science Foundation of China grant: No.81960828 and No.82160862. We thank the associate editor and the reviewers for their useful feedback that improved this paper.

Funding

This work was supported by grants from the National Natural Science Foundation of China(No.81960828 and No.82160862).

Disclosure

The authors declare that they have no conflicts of interest for this work.

References

- Lane CA, Hardy J, Schott JM. Alzheimer's disease [J]. *Eur J Neurol*. 2018;25(1):59–70. doi:10.1111/ene.13439
- Nichols E, Steinmetz JD, Vollset SE. Estimation of the global prevalence of dementia in 2019 and forecasted prevalence in 2050: an analysis for the global burden of disease study 2019 [J]. *Lancet Public Health*. 2022;7(2):e105–e25. doi:10.1016/S2468-2667(21)00249-8
- Plowey ED, Bussiere T, Rajagovindan R, et al. Alzheimer disease neuropathology in a patient previously treated with aducanumab. *Acta Neuropathol*. 2022;144(1):143–153.
- Shinohara M, Tachibana M, Kanekiyo T, et al. Role of LRP1 in the pathogenesis of Alzheimer's disease: evidence from clinical and preclinical studies [J]. *J Lipid Res*. 2017;58(7):1267–1281.
- Li L, Liu J, Yan X, et al. Protective effects of ginsenoside Rd against okadaic acid-induced neurotoxicity in vivo and in vitro [J]. *J Ethnopharmacol*. 2011;138(1):135–141. doi:10.1016/j.jep.2011.08.068
- Zhai L, Pei H, Shen H, et al. Mechanism of neocryptotanshinone in protecting against cerebral ischemic injury: by suppressing M1 polarization of microglial cells and promoting cerebral angiogenesis [J]. *Int Immunopharmacol*. 2023;116:109815. doi:10.1016/j.intimp.2023.109815
- Zhao Y, Long Z, Liu Y, et al. Dihydroartemisinin ameliorates decreased neuroplasticity-associated proteins and excessive neuronal apoptosis in APP/PS1 mice [J]. *Curr Alzheimer Res*. 2020;17(10):916–925. doi:10.2174/1567205017666201215124746
- Tayanloo-Beik A, Kiasalari Z, Roghani M. Paeonol ameliorates cognitive deficits in streptozotocin murine model of sporadic Alzheimer's disease via attenuation of oxidative stress, inflammation, and mitochondrial dysfunction [J]. *J Mol Neurosci*. 2022;72(2):336–348. doi:10.1007/s12031-021-01936-1
- Yang Y, Fu Y, Qin Z, et al. Icaritin improves cognitive impairment by inhibiting ferroptosis of nerve cells. *Aging*. 2023;15(20):11546–11553. doi:10.18632/aging.205144
- Han C, Sheng J, Pei H, et al. Environmental toxin chlorpyrifos induces liver injury by activating P53-mediated ferroptosis via GSDMD-mtROS [J]. *Ecotoxicol Environ Saf*. 2023;257:114938. doi:10.1016/j.ecoenv.2023.114938
- Pei H, He Z, Du R, et al. Imidacloprid activates Kupffer cells pyroptosis to induce liver injury in mice via P2X7 [J]. *Int Immunopharmacol*. 2023;119:110179. doi:10.1016/j.intimp.2023.110179
- Liu N, Zhang T, Sun J, et al. An overview of systematic reviews of Chinese herbal medicine for Alzheimer's disease. *Front Pharmacol*. 2021;12:761661. doi:10.3389/fphar.2021.761661
- Chen SY, Gao Y, Sun JY, et al. Traditional Chinese medicine: role in reducing β -amyloid, apoptosis, autophagy, neuroinflammation, oxidative stress, and mitochondrial dysfunction of Alzheimer's disease. *Front Pharmacol*. 2020;11:497. doi:10.3389/fphar.2020.00497
- Wang M, Pan W, Xu Y, et al. Microglia-mediated neuroinflammation: a potential target for the treatment of cardiovascular diseases [J]. *J Inflamm Res*. 2022;15:3083–3094. doi:10.2147/JIR.S350109
- Huping W, Hongyan W. The effect of Xiaoyao Powder on the behavior, morphology, and neurotransmitter activity of AD model mice [J]. *Chin J Integrated Trad Western Med*. 2014;34(04):471–474.
- Huping W, Hongyan W. Study on the effects of xiaoyao powder on memory function and serum SOD, MDA, ChAT, AchE activities in alzheimer's disease model mice [J]. *Shi Zhen Trad Chin Med*. 2016;27(03):538–540.
- Liu L, Ge F, Yang H, et al. Xiao-Yao-San formula improves cognitive ability by protecting the hippocampal neurons in ovariectomized rats. *Evid Based Complement Alternat Med*. 2020;2020(1):4156145. doi:10.1155/2020/4156145
- Li XH, Zhou XM, Li XJ, et al. Effects of xiaoyaosan on the hippocampal gene expression profile in rats subjected to chronic immobilization stress. *Front Psychiatry*. 2019;10:178. doi:10.3389/fpsy.2019.00178
- Hao W, Wu J, Yuan N, et al. Xiaoyaosan improves antibiotic-induced depressive-like and anxiety-like behavior in mice through modulating the gut microbiota and regulating the NLRP3 inflammasome in the colon. *Front Pharmacol*. 2021;12:619103. doi:10.3389/fphar.2021.619103
- Zhu HZ, Liang YD, Hao WZ, et al. Xiaoyaosan exerts therapeutic effects on the colon of chronic restraint stress model rats via the regulation of immunoinflammatory activation induced by the TLR4/NLRP3 inflammasome signaling pathway. *Evid Based Complement Alternat Med*. 2021;2021:6673538. doi:10.1155/2021/6673538
- Pan T, Shi X, Chen H, et al. Geniposide suppresses interleukin-1 β -induced inflammation and apoptosis in rat chondrocytes via the PI3K/Akt/NF- κ B signaling pathway. *Inflammation*. 2018;41(2):390–399. doi:10.1007/s10753-017-0694-2
- Morsy MA, Abdel-Latif R, Hafez SMNA, et al. Paeonol protects against methotrexate hepatotoxicity by repressing oxidative stress, inflammation, and apoptosis-the role of drug efflux transporters. *Pharmaceuticals*. 2022;15(10):1296. doi:10.3390/ph15101296
- Hu X, Song C, Fang M, et al. Simvastatin inhibits the apoptosis of hippocampal cells in a mouse model of Alzheimer's disease. *Exp Therap Med*. 2018;15(2):1795–1802.
- Erekat NS. Apoptosis and its therapeutic implications in neurodegenerative diseases. *Clin Anat*. 2022;35(1):65–78. doi:10.1002/ca.23792
- Song J, Zhang F, Wang Y, et al. Bak interacts with AKT and is involved in TNF α /CHX-induced apoptosis. *mol Cell Biochem*. 2022;477(3):939–949. doi:10.1007/s11010-021-04348-2
- Kaltschmidt B, Heinrich M, Kaltschmidt C. Stimulus-dependent activation of NF-kappaB specifies apoptosis or neuroprotection in cerebellar granule cells. *Neuromolecular Med*. 2002;2(3):299–309. doi:10.1385/NMM.2.3:299
- Wang HP, Wu HY, Ma CL, et al. Optimal formula of angelica sinensis ameliorates memory deficits in β -amyloid protein-induced Alzheimer's disease rat model. *Curr Med Sci*. 2022;42(1):39–47.
- Shuyun X, Rulian B, Xiu C. *Pharmacological Experimental Methodology*. People's Health Publishing House; 2003.
- Wang M, Bi Y, Zeng S, et al. Modified Xiaoyao San ameliorates depressive-like behaviors by triggering autophagosome formation to alleviate neuronal apoptosis. *Biomed Pharmacother*. 2019;111:1057–1065. doi:10.1016/j.biopha.2018.12.141
- Zhu X, Jing L, Chen C, et al. Danzhi Xiaoyao San ameliorates depressive-like behavior by shifting toward serotonin via the downregulation of hippocampal indoleamine 2,3-dioxygenase. *J Ethnopharmacol*. 2015;160:86–93.
- Tsai PJ, Lai YH, Manne RK, et al. Akt: a key transducer in cancer. *J Biomed Sci*. 2022;29(1):76. doi:10.1186/s12929-022-00860-9
- Wang J, Hu K, Cai X, et al. Targeting PI3K/AKT signaling for treatment of idiopathic pulmonary fibrosis. *Acta Pharm Sin B*. 2022;12(1):18–32. doi:10.1016/j.apsb.2021.07.023
- Jaiswal N, Gavin M, Loro E, et al. AKT controls protein synthesis and oxidative metabolism via combined mTORC1 and FOXO1 signalling to govern muscle physiology. *J Cachexia Sarcopenia Muscle*. 2022;13(1):495–514. doi:10.1002/jcsm.12846

34. Liang W, Xie Z, Liao D, et al. Inhibiting microRNA-142-5p improves learning and memory in Alzheimer's disease rats via targeted regulation of the PTPN1-mediated Akt pathway. *Brain Res Bull.* **2022**;192:107–114. doi:10.1016/j.brainresbull.2022.02.016
35. Yi JH, Baek SJ, Heo S, et al. Direct pharmacological Akt activation rescues Alzheimer's disease like memory impairments and aberrant synaptic plasticity. *Neuropharmacology.* **2018**;128:282–292. doi:10.1016/j.neuropharm.2017.10.028
36. Yuan N, Wang X, Zhang Y, et al. Intervention of NF- κ B signaling pathway and preventing post-operative cognitive dysfunction as well as neuronal apoptosis. *Iran J Public Health.* **2022**;51(1):124–132. doi:10.18502/ijph.v51i1.8303
37. Tsurushima K, Tsubaki M, Takeda T, et al. Dimethyl fumarate induces apoptosis via inhibition of NF- κ B and enhances the effect of paclitaxel and adriamycin in human TNBC cells. *Int J mol Sci.* **2022**;23(15):8681. doi:10.3390/ijms23158681
38. Liu YC, Huang BH, Chung JG, et al. Lenvatinib inhibits AKT/NF- κ B signaling and induces apoptosis through extrinsic/intrinsic pathways in non-small cell lung cancer. *Anticancer Res.* **2021**;41(1):123–130. doi:10.21873/anticancer.14757
39. Zhao X, Huang X, Yang C, et al. Artemisinin attenuates amyloid-induced brain inflammation and memory impairments by modulating TLR4/NF- κ B signaling. *Int J mol Sci.* **2022**;23(11):6354. doi:10.3390/ijms23116354
40. Morgan D, Berggren KL, Spiess CD, et al. Mitogen-activated protein kinase-activated protein kinase-2 (MK2) and its role in cell survival, inflammatory signaling, and migration in promoting cancer. *Mol Carcinog.* **2022**;61(2):173–199. doi:10.1002/mc.23348
41. Gaur R, Mensah KA, Stricker J, et al. CC-99677, a novel, oral, selective covalent MK2 inhibitor, sustainably reduces pro-inflammatory cytokine production. *Arthritis Res Ther.* **2022**;24(1):199. doi:10.1186/s13075-022-02850-6
42. Madani Neishaboori A, Nasser Maleki S, Saberi Pirouz M, et al. Donepezil attenuates injury following ischaemic stroke by stimulation of neurogenesis, angiogenesis, and inhibition of inflammation and apoptosis. *Inflammopharmacology.* **2021**;29(1):153–166. doi:10.1007/s10787-020-00769-5
43. Kim J, Lee HJ, Park SK, et al. Donepezil regulates LPS and A β -stimulated neuroinflammation through MAPK/NLRP3 inflammasome/STAT3 signaling. *Int J mol Sci.* **2021**;22(19):10637. doi:10.3390/ijms221910637
44. Othman MZ, Hassan Z, Che Has AT. Morris water maze: a versatile and pertinent tool for assessing spatial learning and memory [J]. *Exp Anim.* **2022**;71(3):264–280. doi:10.1538/expanim.21-0120

Degenerative Neurological and Neuromuscular Disease

Dovepress
Taylor & Francis Group

Publish your work in this journal

Degenerative Neurological and Neuromuscular Disease is an international, peer-reviewed, open access journal focusing on research into degenerative neurological and neuromuscular disease, identification of therapeutic targets and the optimal use of preventative and integrated treatment interventions to achieve improved outcomes, enhanced survival and quality of life for the patient. The manuscript management system is completely online and includes a very quick and fair peer-review system. Visit <http://www.dovepress.com/testimonials.php> to read real quotes from published authors.

Submit your manuscript here: <http://www.dovepress.com/degenerative-neurological-and-neuromuscular-disease-journal>